Electronic Supplementary Information

Synergistically boosting performances of organic solar cells from dithieno[3,2-*b*]benzo[1,2;4,5-*b'*]dithiophene-based copolymer via side chain engineering and radical polymer additives

Husen Xu,[a‡] Pengzhi Guo,[b‡] Qian Wang,[a*‡]Xin He,[a] Anqi Zhou,[a] Xiaowei Sun,[c] Ergang Wang,[d] Han Young Woo,[e] Hongbin Wu[f] and Yangjun Xia [a*]

[a] Gansu Province Organic Semiconductor Materials and Applied Technology Research Centre, School of Material Science and Engineering, Lanzhou Jiaotong University, Lanzhou 730070, PR China.

[b] National Green Coating Equipment and Technology Research Centre, Lanzhou Jiaotong University, Lanzhou, 730070, P. R. China.

[c] School of Mathematics and Physics, Lanzhou Jiaotong University, Lanzhou 730070, PR China

[d] Department of Chemistry and Chemical Engineering, Chalmers University of Technology, SE-412 96 Göteborg, Sweden.

[e] Department of Chemistry, KU-KIST Graduate School of Converging Science and Technology, Korea University, Seoul 02841, Republic of Korea.

[f] State Key Laboratory of Luminescent Materials and Devices, South China University of Technology, Guangzhou 510640, PR China.

E-mail: WQ739424083@163.com, yjxia73@126.com

‡ These authors contributed equally.

Contents

1 Materials

Unless stated otherwise, all solvents and chemical reagents were obtained commercially and used without further purification. Tris(dibenzylideneacetone) dipalladium ($Pd_2(dba)_3$), tri(o-tolyl)phosphine (P(*o*-tol)$_3$) and 3-chlorothiophene were purchased from Innochem Co., Ltd. 2-(2-butyl octyl)-3-chlorothiophene, 2,7-bis(trimethystannyl)-5,10-di(5-(2-ethylhexyl)-4-chlorothiophen-2yl)dithieno[2,3-;2',3'-*d*′]benzo[1,2-*b*;4,5-*b*′]dithiophene, bis(5-bromothiophen-2-yl)-5,7-bis(2-ethylhexyl)-4H,8H-benzo[1,2-*c*:4,5-*c*′]dithiophene-4,8-dione (BBD) were synthesized according to methods described in previous literature.[1] Dithieno[2,3-*d*;2',3'-*d*′]benzo[1,2-*b*;4,5-*b*′]dithiophene-5,10-diketone was prepared following the procedures in the reported reference. [2]

2 General characterization

^{1}H NMR spectra were recorded on a BRUKER 500 MHz AVANCE NEO spectrometer operating at 500 MHz. Thermogravimetric analysis (TGA) was performed on a TGA 2050 (TA instruments) thermal analysis system at a heating rate of 10 ºC·min^{-1} under nitrogen flow (20 mL·min^{-1}). UV-visible absorption spectra were measured on a UV-1800 spectrophotometer (Shimadzu). Cyclic voltammetry (CV) analysis was performed on a CHI 600D electrochemical workstation (Shanghai Chenhua Co.) at a scan rate of 50 mV/s in a nitrogen-saturated acetonitrile solution containing 0.1 M tetrabutylammonium tetrafluoroborate (Bu_4NPF_6) with glassy carbon electrode and platinum wire as working- and counter-electrode, and $Ag/AgNO_3$ as a reference-electrode. Atomic force microscopy (AFM) measurements (Agilent 5400) were

performed with tapping mode. Transmission electron microscopy (TEM) images were acquired with a Tecnai G2 F20 (FEI, Hillsboro, OR, USA) transmission electron microscope at an accelerating voltage of 200 kV. The GIWAXS measurements were performed at beamline 7.3.3 at the Advanced Light Source. Samples were prepared on Si substrates using identical blend solutions as those used in devices. The 10 keV X-ray beam was incident at a grazing angle of 0.12°–0.16°, selected to maximize the scattering intensity from the samples. The scattered X-rays were detected using a Dectris Pilatus 2M photon counting detector. The film extinction coefficient was calculated by measuring the absorption spectra of polymer films on quartz substrates with different thicknesses. The thickness of the active layer was determined by a DektakXT stylus surface profiler (Bruker Co). The number-average molecular weights (M_n) and the polydispersity index (PDI) of polymers were measured by high-temperature gel permeation chromatography (GPC) with an Agilent PL-GPC220 at 150 °C using 1,2,4-tirchlorobenzene as eluent.

3 Device fabrication and characterization

Before use, the patterned indium tin oxide (ITO) coated glass substrates were cleaned and treated in a UV-Ozone Cleaner for 10 min. PEDOT: PSS (30 nm) was spin-casted on it, and heated at 160 °C for 15 min. Then, the active layer materials (PBDT-Cl: Y6, and PDBT-Cl: Y6; with the weight ratios of the polymer and Y6, 1:0.8, 1:1 to 1:1.2) were spin-coated on the PEDOT: PSS with 1-chloronaphthalene (CN) as solvent additive. After that, the PDINO (in methanol solution) was deposited on top of the active layer by spin-coating, and

then silver was evaporated with a shadow mask as the cathode (100 nm) under vacuum (5×10^{-4} Pa). The thickness of the evaporated cathode was monitored with a quartz crystal thickness/ratio monitor (SI-TM206, Shenyang Sciences Co.). The overlapped area between the cathode and anode defined the pixel size of the device. The device area was measured to be 0.100 ± 0.001 cm^2 with a precision measuring microscope (15J, Shanghai CSOIF Co., Ltd). For the devices with radical conjugated polymer GDTA as additives, the procedure is similar with the devices from pristine polymer: Y6, except that the GDTA solution in chloroform was added before the preparation of the active layer by spin-coating. All the fabrication processes were carried out under a controlled atmosphere in a nitrogen dry box (Etelux Co.) containing less than 1 ppm oxygen and moisture.

The current density-voltage (*J-V*) characteristics of the OSCs were measured in a glovebox with a Keithley 2400 measuring unit under 1 sun, AM1.5G spectra (100 $mW \cdot cm^{-2}$) from a solar simulator (XES-70S1, San-EI Electric Co). The light intensity was calibrated with a 20 mm × 20 mm monocrystalline silicon reference cell (SF-3, SOFN Instruments Co., Ltd.). The *J-V* curves were measured along the forward scan direction from − 0.2 to 1.0 V, with a scan step of 20 mV with a delay time of 0.1 seconds. The EQE was measured with a commercial EQE/incident photon to charge carrier efficiency (IPCE) setup (7-SCSpecIII, Beijing 7-star Opt. In. Co.), in which an integrated standard single-crystal Si photovoltaic cell (S1337-101BQ, SOFN instruments co., Ltd.

calibrated by National Institute of Metrology of China) was employed to calibrate the light intensity at each wavelength.

4 Molecular dynamics simulations

The molecular dynamics (MD) simulations were carried out following the procedure described by Tang et al.[3] using the Materials Studio 6.0 package. The force field used was the Compass force field. The BHJ active systems based on Y6 mixed with different polymers were simulated by cubic cells, and in each cell, there were 5 polymer molecules, and each polymer model consisted of 10 repeating units. The numbers of the acceptor molecules put in the cells were determined from the donor: acceptor weight ratios used for fabricating the corresponding solar cells. The initial simulations were carried out by randomly placing the polymers and the acceptor molecules in the cells with a very low density (0.1 g·cm^{-3}). The corresponding construction process was done using Amorphous Cell package in Materials Studio, and the ring spearing and close contacts were examined.

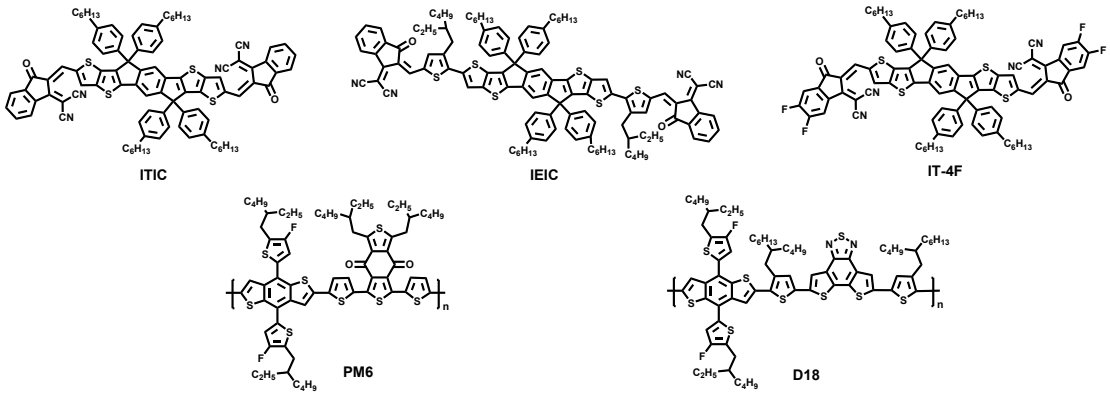

Fig. S1 Chemical structures of the mentioned small molecular acceptors and polymer donors.

Table S1. Summary of the energy loss in the NFA-OSCa from BDT and DTBDT unit-based polymer donors

	Active layer	V_{OC} (V)	J_{SC} (mA/cm^2)	FF (%)	PCE (%)	E_g-eV_{OC} (eV)	Ref.		Active layer	V_{OC} (V)	J_{SC} (mA/cm^2)	FF (%)	PCE (%)	E_g-eV_{OC} (eV)	Ref.
NFA-OSCs from BDT-based polymer donors	J52-Cl:F-BTA3	1.15	12.81	68.55	10.10	0.62	4	**NFA-OSCs from DTBDT-based polymer donors**	PE52:F-BTA3	1.14	10.53	56.49	6.78	0.63	4
	PM6:IT-4F	0.84	22.20	72.50	13.50	0.78	5		PDBT-F:IT-4F	0.81	20.90	59.00	10.90	0.81	6
	PM6:IDIC	0.97	17.80	69.00	11.90	0.81	7		PDBT-F:IDIC	0.87	17.65	71.50	11.02	0.91	8
	PM7:IT-4F	0.85	20.50	76.80	13.40	0.77	9		PDBT-Cl:IT-4F	0.82	22.30	69.00	12.60	0.80	6
	PM6:IT-M	1.02	15.80	58.43	9.42	0.58	10		PDBT-F:IT-M	0.97	17.02	63.71	10.52	0.63	8
	J52-Cl:Y6	0.84	23.77	61.44	12.31	0.62	11		PE52:Y6	0.80	25.36	71.94	14.61	0.66	12
	D18-Cl:BTA3	1.30	8.29	58.43	6.30	0.59	13		PE55:BTA3	1.28	11.06	64.20	9.36	0.61	13

5 Synthesis

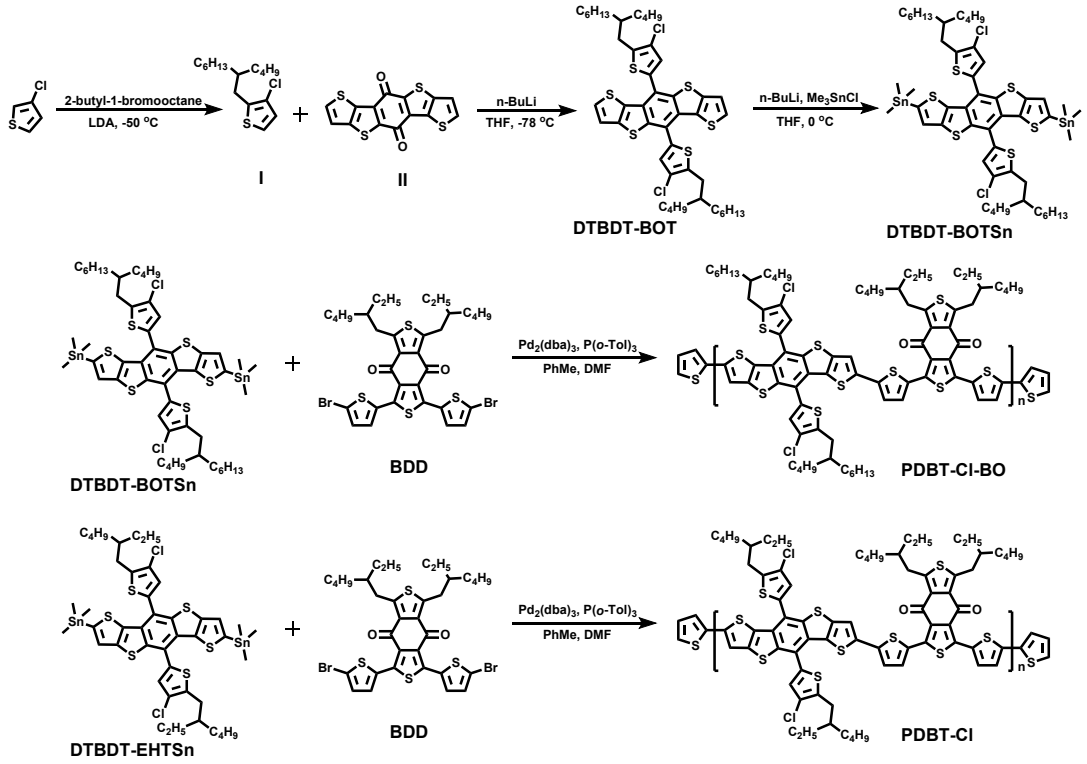

Scheme S1. Synthetic route of the monomers and polymers

DTBDT-BOT: In a three-neck flask equipped with a condenser, stirring bar and a nitrogen-filled balloon, 2-(2-butyloctyl)-3-chlorothiophene (2.98 g, 10.4 mmol), 50 mL anhydrous THF was injected through a syringe. After the solution in the flask was cooled to −20 °C for 30 minutes, 5.4 mL n-BuLi (2.5 M) in hexane was added dropwise and stirred for another 2 h. Then, the balloon was replaced with nitrogen flow, and the solution was heated to 50°C. Dithieno[2,3-*d*;2',3'-*d'*]benzo[1,2-*b*;4,5-*b'*]dithiophene-5,10-diketone (1.10 g, 3.3 mmol) was added in one portion, and the reaction was kept at 50 °C under vigorous stirring for 1 h. After that, a solution of 20% hydrochloric acid containing 5 g stannous chloride dihydrate was then added, and the reaction was carried on overnight. The reaction was extracted with chloroform (50 mL) three times.

Subsequently, the combined organic phase was dried by anhydrous $MgSO_4$, and the solvent was removed by rotary evaporation under reduced pressure. The light-yellow oil-like residues was purified by column chromatography with n-hexane as eluent, and DTBDT-BO (1.84 g, Yield of 64%) was obtained. ^{1}H NMR (500 MHz, $CDCl_3$) δ (ppm): 7.43 (d, J = 5 Hz, 1H), 7.27 (d, J = 5 Hz, 1H), 7.14 (s, 1H), 2.91 (d, J = 5 Hz, 2H), 1.85−1.80 (m, 1H), 1.43−1.31 (m, 16H), 0.94−0.87 (m, 6H).

DTBDT-BOTSn: In a one-neck flask equipped with a stirring bar, DTBDT-BOT (1.50 g, 1.72 mmol) was added. Then, the flask related to a vacuum pump through a vacuum glass airway, and heated by a heat gun for 10 min. After that, the vacuum pump was removed, and a nitrogen-filled balloon was connected. 50 ml anhydrous THF was added, and the solution was cooled to −78 ℃. Subsequently, 2.10 mL n-butyllithium (2.5 M in hexane) was added dropwise, and the reaction continued for 2 h. Finally, a solution of trimethyl tin chloride (1.04 g, 5.22 mmol) in hexane was added and the reaction was continued at −78 ℃ for another 2 h, and then kept at ambient temperature under stirring overnight. After quenched with distilled water, the resulting mixture was extracted with ethyl acetate (60 mL) three times and the combined organic phase was dried by anhydrous $MgSO_4$ and concentrated to obtain coarse product. Column chromatography separation and purification (neutral alumina as stationary phase, petroleum ether as fluidity), recrystallization to obtain yellowish solid (0.95 g, 46%). ^{1}H NMR (500 MHz, $CDCl_3$) δ (ppm): 7.27 (s, 1H), 7.14 (s, 1H), 2.93 (d, J = 5 Hz, 2H), 1.93−1.79 (m, 2H), 1.45−1.21 (m, 41H), 0.91−0.81 (m, 12H), 0.45−0.33 (m, 9H).

PDBT-Cl-BO: DTBDT-BOTSn (180 mg, 0.15 mmol), brominated monomer BDD

(115 mg, 0.15 mmol), $Pd_2(dba)_3$ (1.5 mg), and P(*o*-tolyl)$_3$ (3.0 mg) were dissolved in dry toluene. Under nitrogen protection, the reaction mixture was stirred at 100 °C for 12 h. Finally, the termination reaction with the 2-tributylstannylthiophene and 2-bromothiohene was successively implemented. After the reaction solution was cooled to ambient temperature. The solution was dropped into 200 mL methanol. Then the precipitation was collected and extracted with methanol, n-hexane and chloroform in a Soxhlet extractor. The polymer solution in chloroform was concentrated and dropped into methanol again. The resulting polymer was dried under vacuum to give a red grass-like powder of 164 mg (yield: 74%). M_n = 57.2 kDa、M_w = 97.4 kDa、PDI = 1.7.

PDBT-Cl: The PDBT-Cl was prepared with a similar procedure as the PDBT-Cl-BO with a yield of 77%. M_n = 31.2 kDa、M_w = 82.2 kDa、PDI = 2.6.

6 ^{1}H NMR spectra of the monomers

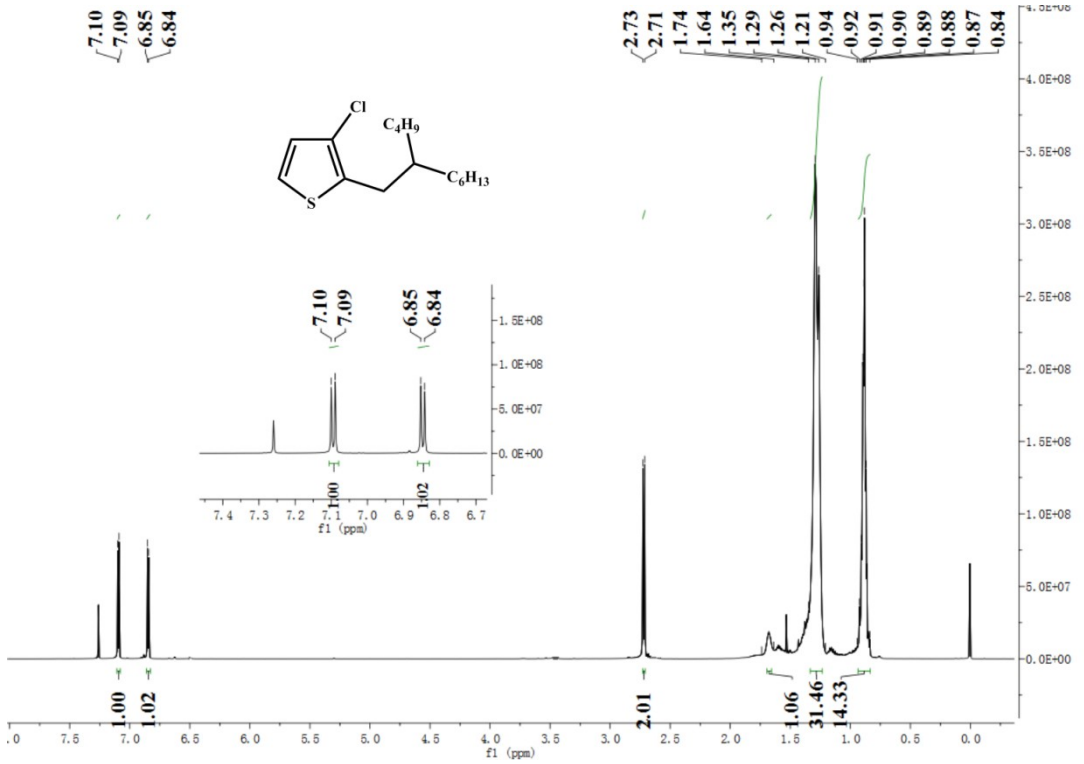

Fig. S2. ^{1}H NMR spectrum of compound **I** in $CDCl_3$.

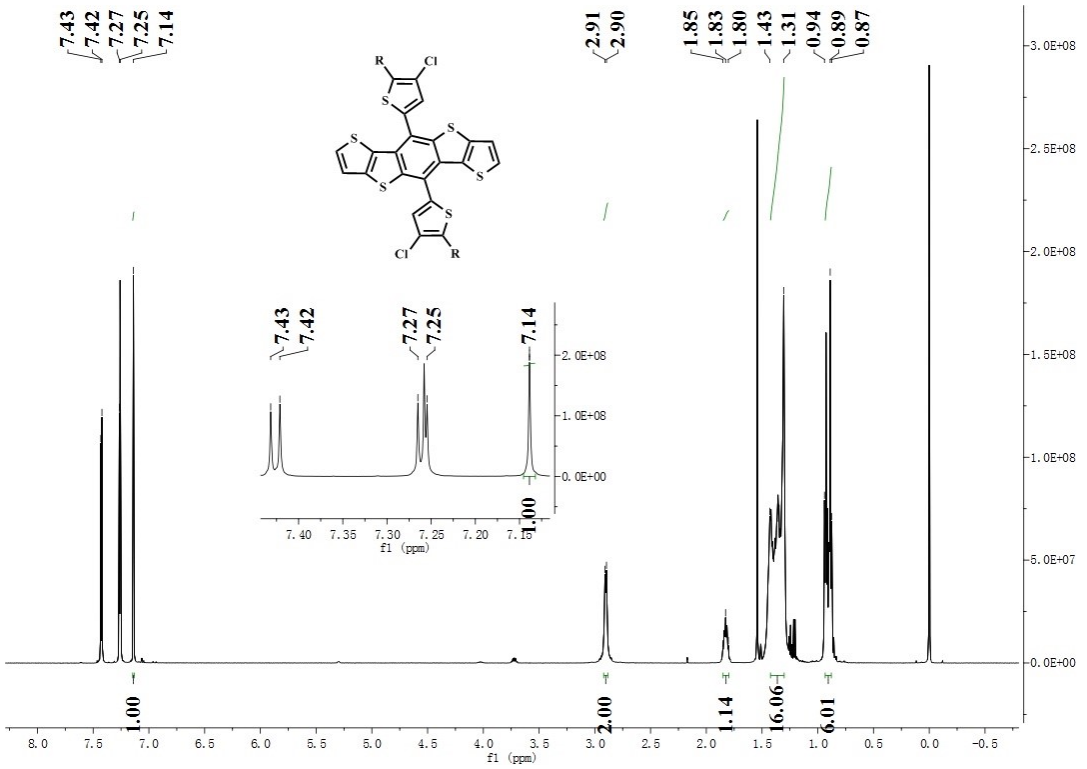

Fig. S3. ^{1}H NMR spectrum of DTBDT-BOT in $CDCl_3$.

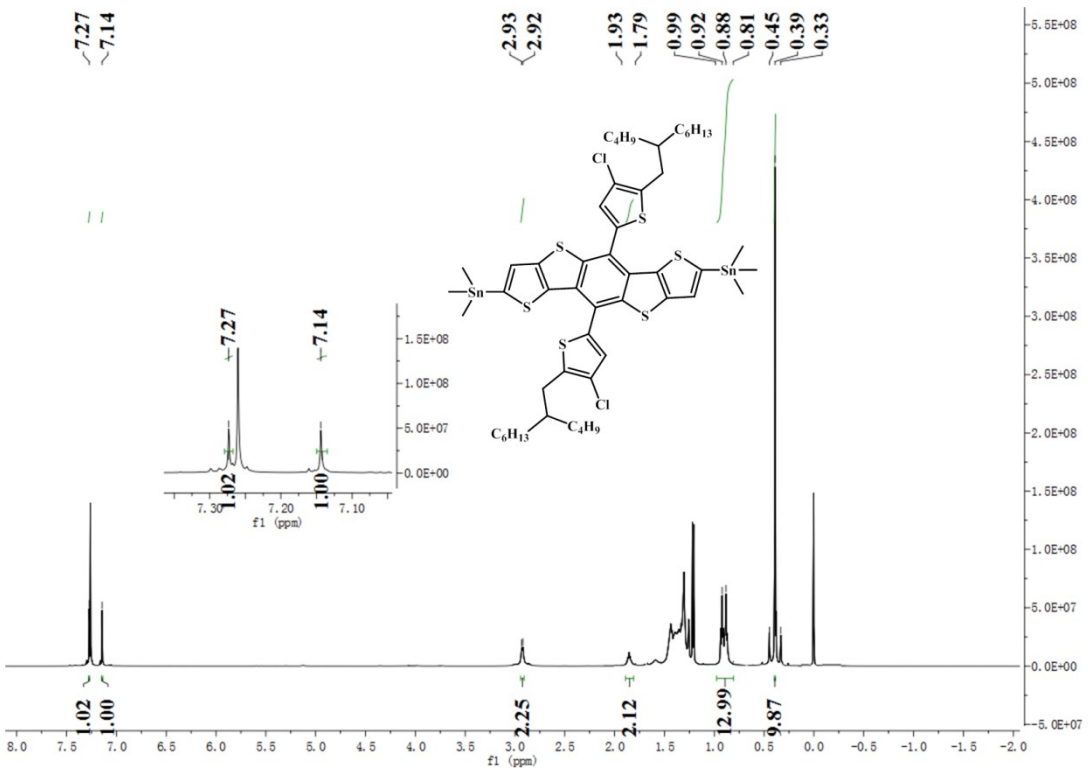

Fig. S4. ^{1}H NMR spectrum of DTBDT-BOTSn in $CDCl_3$.

7 Thermogravimetric curves of the polymers

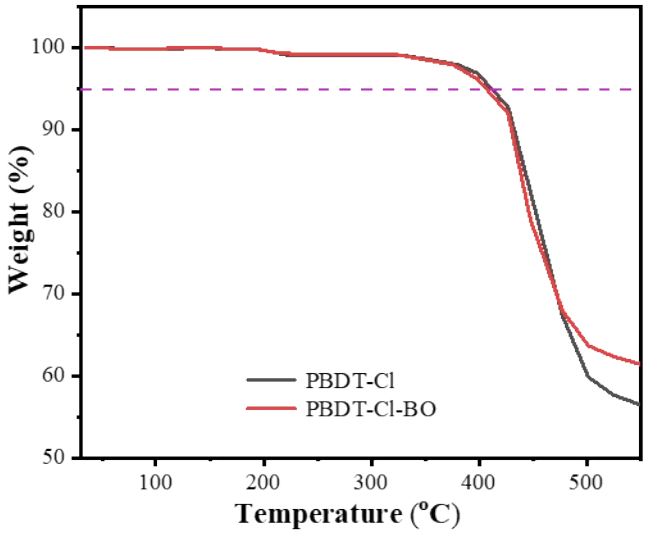

Fig. S5. TG curves of PDBT-Cl and PDBT-Cl-BO.

8 Optical and electrochemical characterizations

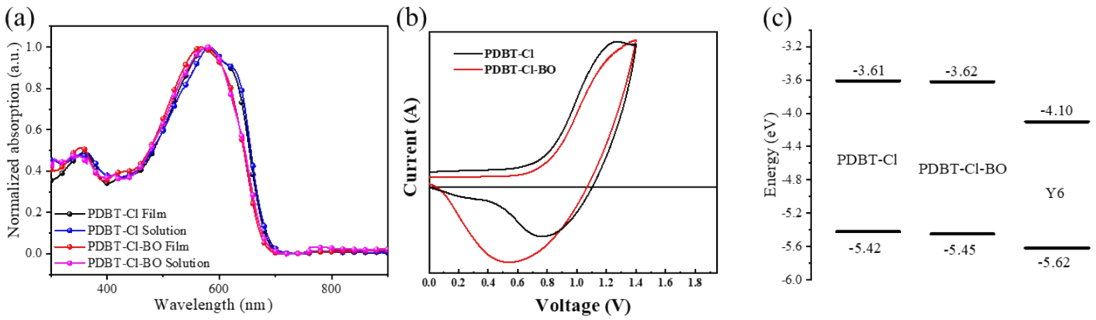

Fig. S6. Normalized absorption spectra of PDBT-Cl and PDBT-Cl-BO in solid state and CB solution (a). Cyclic voltammetry curves of PDBT-Cl and PDBT-Cl-BO films (b). Energy-level diagram of PDBT-Cl, PDBT-Cl-BO and Y6 (b).

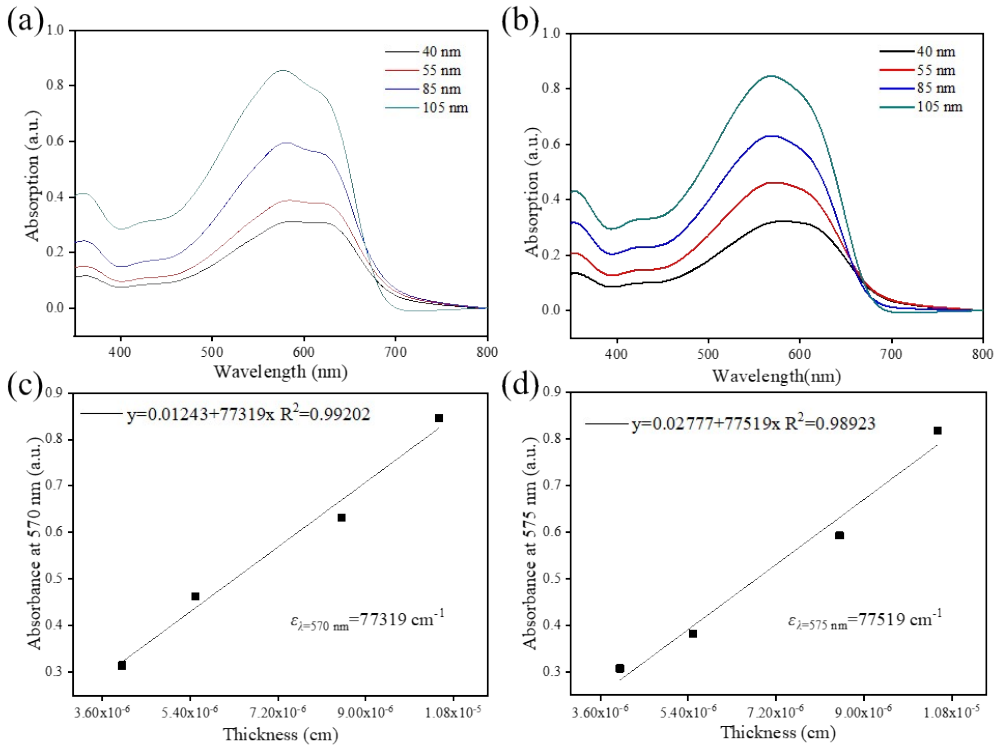

Fig. S7. Film absorption (a), (b) and extinction coefficient (c), (d) of PDBT-Cl (a), (c) and PDBT-Cl-BO (b), (d).

9 Charge mobility of the pristine and blend films

The charge transfer properties of blend films based on PDBT-Cl: Y6 and /or /PDBT-Cl-BO: Y6 were evaluated using the space-charge-limited current (SCLC) method on the hole-only devices with configuration as ITO/PEDOT:PSS/polymer: Y6/MoO_3/Ag. The mobility was determined by fitting the dark current to the model of a single-carrier SCLC. According to Mott-Gurney's square law, it is calculated by the following fitting formula：

$$\mu = \frac{8L^3 \ J}{9\varepsilon_0\varepsilon_r V^2}$$

where J is the current density, μ is the zero-field mobility of holes (μ_h), ε_0 is the permittivity of the vacuum, ε_r is the relative permittivity of the material, L is the thickness of the blend film, and V is the effective voltage ($V = V_{appl} - V_{bi}$, where V_{appl} is the applied voltage, and V_{bi} is the built-in potential determined by electrode work function difference). The mobility was calculated from the slope of $J^{1/2}$-V plots.

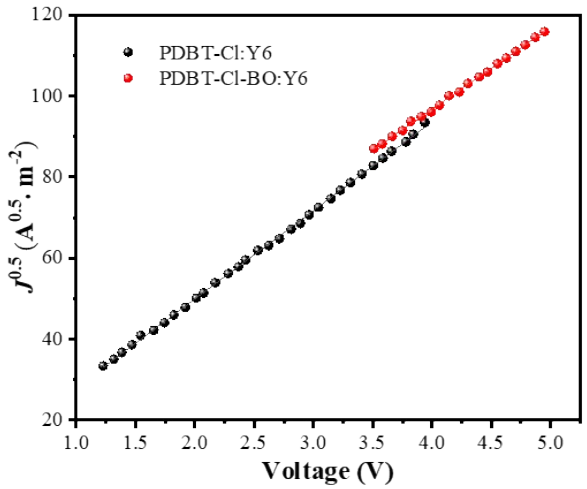

Fig. S8. *J-V* characteristics of hole-only devices based on polymer: Y6 blend films.

10 Temperature depended absorption

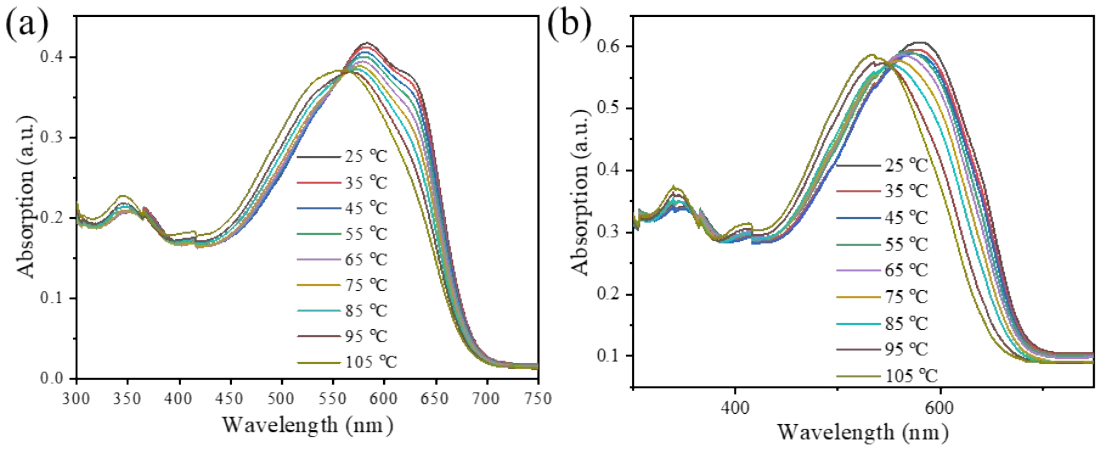

Fig. S9. Temperature depended absorption of PDBT-Cl (a) and PDBT-Cl-BO (b) in CB solvent.

11 GIWAXS parameters

Table S2. Structural parameters of the pristine and optimal blend films of PDBT-Cl, and PDBT-Cl-BO obtained from the GIWAXS measurements

Film	(100)		(010) of polymer		(010) of Y6	
	Q_{xy}/Q_z (Å^{-1})	d-spacing (Å)	Q_{xy}/Q_z (Å^{-1})	*d*-spacing (Å)	Q_z (Å^{-1})	d-spacing (Å)
PDBT-Cl	–/0.347	–/18.10	1.564/1.576	4.01/3.98	–	–
PDBT-Cl-BO	0.291/0.362	21.58/17.35	1.537/1.645	4.08/3.82	–	–
PDBT-Cl: Y6	0.296/0.345	21.22/18.20	1.524/1.524	4.12/4.12	1.758	3.57
PDBT-Cl-BO: Y6	0.296/0.368	21.22/17.06	1.512/–	4.15/–	1.804	3.48

12 FTPS-EQE and EL measurements

FTPS measurements were carried out following the procedure described by Cao et al.[14] using a Nicolet iS50 (Thermo Scientific) with an external detector option.[15] Photocurrents generated from the solar cells were amplified by a low-noise current amplifier (SR570) with light modulated by the Fourier transform infrared spectroscope (FTIR). The electroluminescence (EL) spectra were acquired by a spectroradiometer (PR745, Photo Research) or a high-sensitivity spectrometer (QE Pro or NIR Quest 512, Ocean Optics). The radiation flux of EL was determined by measuring the emitted photons in all directions through an integrated sphere by using calibrated spectrometers (QE Pro, and NIRQuest-512, Ocean Optics), under a constant current density with a Keithley 2400 source measure unit. Calibration for EL: Before collecting the radiant flux from the organic solar cells, the spectrometer was calibrated by a standard halogen calibration light source (HL-3-plus-INT-CAL). The irradiance of the light source in 350−2400 nm was determined to be with the maximum uncertainty level of 7%. The calibration was accomplished by using the following procedure: i) The output diffusor of HL-3 light source was placed at the aperture of integrating sphere, which was connected to the QE-Pro spectrometer by a fiber; ii) A dark spectrum was recorded to minimize the influence of a shifted dark spectrum; iii) The lamp was turned on and allowed to warm up for at least 15 minutes before use; iv) The calibration files that came with the HL-3-plus-INT-CAL light source were input into the spectrometer operating software.

Fourier transform photocurrent spectroscopy (FTPS-EQE) and Electroluminescence spectra (EL) were used to characterize the external quantum efficiency of the two devices, and the voltage loss of the two blended systems was quantified. The optical band gap (E_g) of the two systems is determined by the intersection of the FTPS-EQE and EL spectra. The radiative recombination energy loss ($\triangle V_{rad}$) can be calculated according to the formula below:

$$\triangle V_{OC}^{rad} = \frac{E_g}{q} - \triangle V_{OC}^{SC} - V_{OC}^{rad}$$

Where V_{OC}^{rad} is the upper limit of the open-circuit voltage in the presence of radiative recombination only ($V_{OC}^{rad} = \frac{KT}{q} ln(\frac{J_{sc}}{J_0^{rad}})$), K is Boltzmann's constant, q is the amount of elementary charge, T is the absolute temperature.[16]

Non-radiative recombination loss can be calculated by electroluminescence and defined as:

$$\triangle V_{OC}^{non-rad} = V_{oc}^{rad} - V_{OC} = -\frac{KT}{q} ln(EQE_{EL})$$

Where EQE_{EL} is the external quantum efficiency of electroluminescence ($EQE_{EL} = \frac{J_{em}(V)}{J_{inj}(V)}$), $J_{em}(V)$ is the radiative emission current and $J_{inj}(V)$ is the current injected in the dark by the applied voltage bias V.[16,17] The energy loss calculation results of organic solar cells are summarized in Table 3.

13 Exciton dissociation of blend films

Table S3. Exciton dissociation probability behaviors of NFA-OSCs based on optimized PDBT-Cl: Y6 and PDBT-Cl-BO: Y6 blend films with and without GDTA

Active Layer	J_{sat} (mA·cm^{-2})	*P(E,T)*
PDBT-Cl:Y6 =1:1.2 + w/o	25.00	96.68%
PDBT-Cl:Y6 =1:1.2 +2% GDTA	26.64	96.84%
PDBT-Cl-BO:Y6 =1:1.2 + w/o	25.67	97.38%
PDBT-Cl-BO:Y6 =1:1.2 +2% GDTA	26.80	97.65%

Table S4. The photovoltaic performances of the OSCs from typical DTBDT-based polymers

Active layer	V_{OC} (V)	J_{SC} (mA/cm^2)	FF (%)	PCE (%)	Ref.
PDTBDDR-BZ : $PC_{71}BM$	0.62	6.36	48.10	1.91	18
PDTBDAT-BZ : $PC_{71}BM$	0.80	9.38	67.81	5.10	18
PDT-S-T : $PC_{71}BM$	0.73	16.63	64.13	7.79	19
PBT-HD-DPP-C16 : $PC_{71}BM$	0.62	6.41	60.9	2.42	20
PBT-T-DPP-C12 : $PC_{71}BM$	0.65	12.61	63.4	5.19	20
PBT-TIPS-DPP-C16 : $PC_{71}BM$	0.75	13.9	61.3	6.39	20
pDTBDT-DTPD : $PC_{71}BM$	0.79	6.64	53.9	2.83	21
pDTBDT-TTEH : $PC_{71}BM$	0.72	15.77	59.4	6.74	21
PDTP-DTBDT : $PC_{71}BM$	0.83	15.10	54.3	6.81	22
PDBT-T1 : SdiPBI-S	0.90	11.98	66.1	7.16	23
PDBT-T1 : $PC_{71}BM$	0.92	14.11	75.0	9.74	24
PDBT-T1 : TN-PDI	0.95	7.52	40.0	3.00	25

PDTBDT-T-3T : $PC_{71}BM$	0.62	10.65	66.51	4.39	26
PDTBDT-BZ : $PC_{71}BM$	0.83	10.28	64.9	5.54	27
PDTBDT-FBTz : $PC_{71}BM$	0.95	9.32	62.7	5.55	28
P(DTBDAT-TCNT) : $PC_{71}BM$	0.77	12.2	62.0	5.83	29
PDTBDT-BZF2 : $PC_{71}BM$	0.98	12.76	59.6	7.45	28
PDBT-T1 : IC-C6IDT-IC	0.89	15.05	65.0	8.71	30
PDBT-T1 : ITIC-Th	0.88	16.24	67.1	9.60	31
PDBT-T1 : Alloy	0.90	14.9	74.4	10.00	32
PDBT-T1 : SdiPBI-Se : ITIC-Th	0.93	15.37	70.2	10.27	33
PzIIG-BTT2TC10 : $PC_{71}BM$	0.94	5.89	60.78	3.36	34
PDBT-T1 : P4N4	0.96	9.40	63.4	5.71	35
PDTBDT-BT : $PC_{71}BM$	0.82	15.20	68.5	8.54	36
PDTBDT-FBT : $PC_{71}BM$	0.91	14.89	64.5	8.74	36
PTzBI-DT : ITIC	0.91	16.84	61.53	9.43	37
PDBT-T1 : $PC_{71}BM$: ITIC-Th	0.93	15.54	70.5	10.48	38
PDBT-T1 : BPT	1.00	11.08	63.2	7.16	39
PDBT-T1 : BPT-S	1.02	11.94	68.1	8.28	39
PDTBDT-TPT1 :ITIC	0.94	13.19	61.1	7.58	40
PDBT-DTT : ITCPTC	0.79	15.6	68.2	8.74	41
DTBDT-TzVTz : $PC_{71}BM$	0.79	13.17	64.0	6.73	42
PDBT-F : $PC_{71}BM$	0.93	12.63	61.96	7.28	8
PDBT-F : IDIC	0.87	17.65	71.5	11.02	8
PDBT-F : IDIC : $PC_{71}BM$	0.89	18.69	70.88	11.86	8
PDBT-T1 : PPDI-Se	1.05	10.7	66.3	7.47	43
PDBT-T1 : PM-PDI3	0.98	11.02	69.9	7.58	44
PDBT(E)BTz-*d* : IT-4F	0.95	15.44	54.5	7.81	45
PDBT-Cl : IT-4F	0.82	22.3	69.0	12.6	6
PE52 : F-BTA3	1.14	10.53	56.49	6.78	4

PDTBDT : Y6	0.895	17.18	53.50	8.22	46
PDTBDT-T : Y6	0.780	24.21	65.81	12.71	46
PDTBDT-T-Cl : Y6	0.860	24.46	71.65	15.63	46
PE64 : ITIC	0.79	12.43	48.0	4.69	49
PE64 : Y6	0.50	14.05	50.0	3.54	49
PE65 : ITIC	0.94	14.40	67.0	9.13	49
PE65 : Y6	0.77	25.20	67.0	13.01	49
PDTBDT-TS-DPP : $PC_{71}BM$	0.71	16.21	71.03	8.17	50
PDTBDT-T-DPP : $PC_{71}BM$	0.68	12.70	67.10	5.79	50
PE51 : Y6	0.79	24.11	69.75	13.34	12
PE52 : Y6	0.80	25.36	71.94	14.61	12
PE53 : Y6	0.83	23.64	69.84	13.72	12
PE55 : Y6	0.82	25.55	71.44	15.00	47
PE56 : Y6	0.86	25.88	72.70	16.11	47
PE55 : BTA3	1.28	11.06	64.20	9.36	13
PE52 : Y18	0.83	26.26	74.02	16.13	48

Reference

1. S. Zhang, Y. Qin, J. Zhu and J. Hou, *Adv. Mater.*, 2018, **30**, 1800868.
2. P. Gao, D. Beckmann, H. N. Tsao, X. Feng, V. Enkelmann, M. Baumgarten, W. Pisula and K. Müllen, *Adv. Mater.*, 2009, **21**, 213−216.
3. J. Wang, X. Jiang, H. Wu, G. Feng, H. Wu, J. Li, Y. Yi, X. Feng, Z. Ma, W. Li, K. Vandewal and Z. Tang, *Nat. Commun.*, 2021, **12**, 6679.
4. T. Dai, P. Lei, B. Zhang, J. Zhou, A. Tang, Y. Geng, Q. Zeng and E. Zhou, *ACS Appl. Mater. Interfaces* 2021, **13**, 30756−30765.

5. Q. Fan, W. Su, Y. Wang, B. Guo, Y. Jiang, X. Guo, F. Liu, T. P. Russell, M. Zhang and Y. Li, *Sci. China Chem.*, 2018, **61**, 531–537.

6. J. Huang, L. Xie, L. Hong, L. Wu, Y. Han, T. Yan, J. Zhang, L. Zhu, Z. Wei and Z. Ge, *Mater. Chem. Front.*, 2019, **3**, 1244–1252.

7. Q. Fan, Y. Wang, M. Zhang, B. Wu, X. Guo, Y. Jiang, W. Li, B. Guo, C. Ye, W. Su, J. Fang, X. Ou, F. Liu, Z. Wei, T. C. Sum, T. P. Russell and Y. Li, *Adv. Mater.,* 2018, **30**, 1704546.

8. J. Huang, R. Peng, L. Xie, W. Song, L. Hong, S. Chen, Q. Wei and Z. Ge, *J. Mater. Chem. A*, 2019, **7**, 2646–2652.

9. M.-A. Pan, T.-K. Lau, Y. Tang, Y.-C. Wu, T. Liu, K. Li, M.-C. Chen, X. Lu, W. Ma and C. Zhan, *J. Mater. Chem. A*, 2019, **7**, 20713–20722.

10. J. Gao, X. Ma, C. Xu, X. Wang, J. H. Son, S. Y. Jeong, Y. Zhang, C. Zhang, K. Wang, L. Niu, J. Zhang, H. Y. Woo, J. Zhang and F. Zhang, *Chem. Eng. J.*, 2022, **428**, 129276.

11. A. Tang, Q. Zhang, M. Du, G. Li, Y. Geng, J. Zhang, Z. Wei, X. Sun and E. Zhou, *Macromolecules,* 2019, **52**, 6227–6233.

12. J. Zhou, B. Zhang, M. Du, T. Dai, A. Tang, Q. Guo and E. Zhou, *Nanotechnology*, 2021, **32**, 225403.

13. X. Li, Z. Wang, A. Tang, Q. Guo, Y. Liu, M. Du and E. Zhou, *Macromol. Rapid Commun.*, 2023, **44**, 2300019.

14. S. Liu, J. Yuan, W. Deng, M. Luo, Y. Xie, Q. Liang, Y. Zou, Z. He, H. Wu and Y. Cao, *Nat. Photonics.,* 2020, **14**, 300.

15. K. Vandewal, K. Tvingstedt, A. Gadisa, O. Inganas, J.V. Manca, *Nat. Mater.*, 2009, **8**, 904.

16. U. Rau, B. Blank, T. C. M. Müller and T. Kirchartz, *Phys. Rev. Appl.*, 2017, **7**, 044016.

17. U. Rau, *Phys. Rev. B*, 2007, **76**, 085303.

18. H.J. Yun, Y.J. Lee, S.J. Yoo, D.S. Chung, Y.H. Kim and S.K. Kwon, *Chem. Eur. J.*, 2013, **19**, 13242-13248.

19. Y. Wu, Z. Li, W. Ma, Y. Huang, L. Huo, X. Guo, M. Zhang, H. Ade and J. Hou, *Adv. Mater.*, 2013, **25**, 3449-3455.

20. S. Sun, P. Zhang, J. Li, Y. Li, J. Wang, S. Zhang, Y. Xia, X. Meng, D. Fan and J. Chu, *J. Mater. Chem. A.*, 2014, **2**, 15316-15325.

21. N. Shin, H.J. Yun, Y. Yoon, H.J. Son, S.Y. Ju, S.K. Kwon, B.S. Kim and Y.H. Kim, *Macromolecules.*, 2015, **48**, 3890-3899.

22. Y. JináKim, T. KyuáAn and C. EonáPark, *Chem. Commun.*, 2015, **51**, 11572-11575.

23. D. Sun, D. Meng, Y. Cai, B. Fan, Y. Li, W. Jiang, L. Huo, Y. Sun and Z. Wang, *J. Am. Chem. Soc.*, 2015, **137**, 11156-11162.

24. L. Huo, T. Liu, X. Sun, Y. Cai, A.J. Heeger and Y. Sun, *Adv. Mater.*, 2015, **27**, 2938-2944.

25. Y. Cai, X. Guo, X. Sun, D. Wei, M. Yu, L. Huo and Y. Sun, *Sci. China.: Chem.*, 2016, **59**, 427-434.

26. J. Li, X. Wang, S. Du, J. Tong, P. Zhang, P. Guo, C. Yang and Y. Xia, *J Macromol Sci A.*, 2016, **53**, 538-545.

27. H.S. Lee, H.G. Song, H. Jung, M.H. Kim, C. Cho, J.Y. Lee, S. Park, H.J. Son, H-J. Yun, S-K. Kwon, Y-H. Kim and B. Kim, *Macromolecules.*, 2016, **49**, 7844-7856.

28. W. Zhong, J. Xiao, S. Sun, X.F. Jiang, L. Lan, L. Ying, W. Yang, H.L. Yip, F. Huang and Y. Cao, *J. Mater. Chem. C.*, 2016, **4**, 4719-4727.

29. Y.S. Lee, S.Song, Y.J. Yoon, Y.J. Lee, S.K. Kwon, J.Y. Kim and Y.H. Kim, *J. Polym. Sci. Pol. Chem.*, 2016, **54**, 3182-3192.

30. Y. Lin, Q. He, F. Zhao, L. Huo, J. Mai, X. Lu, C. Su, T. Li, J. Wang, J. Zhu, Y. Sun, C. Wang and X. Zhan, *J. Am. Chem. Soc.*, 2016, **138**, 2973-2976.

31. Y. Lin, F. Zhao, Q. He, L. Huo, Y. Wu, T. Parker, W. Ma, Y. Sun, C. Wang, D. Zhu, A.J. Heeger, S.R. Marder and X. Zhan, *J. Am. Chem. Soc.*, 2016, **138**, 4955-4961.

32. P. Cheng, C. Yan, Y. Wu, J. Wang, M. Qin, Q. An, J. Cao, L. Huo, F. Zhang, L. Ding, Y. Sun, W. Ma and X. Zhan, *Adv. Mater.*, 2016, **28**, 8021-8028.

33. T. Liu, Y. Guo, Y. Yi, L. Huo, X. Xue, X. Sun, H. Fu, W. Xiong, D. Meng, Z. Wang, F. Liu, T.P. Russell and Y. Sun, *Adv. Mater.*, 2016, **28**, 10008-10015.

34. J.L. Li, Y.F. Chai, W.V. Wang, Z.F. Shi, Z.G. Xu and H.L. Zhang, *Chem. Commun.*, 2017, **53**, 5882-5885.

35. X. Liu, T. Liu, C. Duan, J. Wang, S. Pang, W. Xiong, Y. Sun, F. Huang and Y. Cao, *J. Mater. Chem. A.*, 2017, **5**, 1713-1723.

36. P. Guo, G. Luo, Q. Su, J. Li, P. Zhang, J. Tong, C. Yang, Y. Xia and H. Wu, *ACS Appl. Mater. Interfaces.*, 2017, **9**, 10937-10945.

37. B. Fan, K. Zhang, X.F. Jiang, L. Ying, F. Huang and Y. Cao, *Adv. Mater.*, 2017, **29**, 1606396.

38. T. Liu, X. Xue, L. Huo, X. Sun, Q. An, F. Zhang, T.P. Russell, F. Liu and Y. Sun, *Chem. Mater.*, 2017, **29**, 2914-2920.

39. Z. Luo, T. Liu, W. Cheng, K. Wu, D. Xie, L. Huo, Y. Sun and C. Yang, *J. Mater. Chem. C.*, 2018, **6**, 1136-1142.

40. P. Gao, J. Tong, P. Guo, J. Li, N. Wang, C. Li, X. Ma, P. Zhang, C. Wang and Y. Xia, *J. Polym. Sci. Pol. Chem.*, 2018, **56**, 85-95.

41. Y. Cai, X. Xue, G. Han, Z. Bi, B. Fan, T. Liu, D. Xie, L. Huo, W. Ma, Y. Yi, C. Yang and Y. Sun, *Chem. Mater.*, 2018, **30**, 319-323.

42. J. Hong, C. Wang, H. Cha, H.N. Kim, Y. Kim, C.E. Park, T.K. An, S.K. Kwon and Y. H. Kim, *Chem. Eur. J.*, 2019, **25**, 649-656.

43. G. Li, S. Yang, T. Liu, J. Li, W. Yang, Z. Luo, C. Yan, D. Li, X. Wang, G. Cui, T. Yang, L. Xu, S-Z. Zhan, L. Huo, H. Yan and B. Tang, *J. Mater. Chem. C.*, 2019. **7**, 14563-14570.

44. G. Li, W. Yang, S. Wang, T. Liu, C. Yan, G. Li, Y. Zhang, D. Li, X. Wang, P. Hao, J. Li, L. Huo, H. Yan and B. Tang, *J. Mater. Chem. C.*, 2019, **7**, 10901-10907.

45. D. Liu, Y. Zhang, L. Zhan, T.K. Lau, H. Yin, P.W. Fong, S.K. So, S. Zhang, X. Lu, J. Hou, H. Chen, W.Y. Wong and G. Li, *J. Mater. Chem. A.*, 2019, **7**, 14153-14162.

46. Y. Tang, L. Xie, D. Qiu, C. Yang, Y. Liu, Y. Shi, Z. Huang, J. Zhang, J. Hu, K. Lu and Z. Wei, *J. Mater. Chem. C.*, 2021, **9**, 7575-7582.

47. J. Zhou, Q. Guo, B. Zhang, S.X. Cheng, X.T. Hao, Y. Zhong, A. Tang, X. Sun and E. Zhou, *ACS Appl. Mater. Interfaces.*, 2022, **14**, 52244-52252.

48. M. Du, A. Tang, J. Yu, Y. Geng, Z. Wang, Q. Guo, Y. Zhong, S. Lu and E. Zhou, *Adv. Mater.*, 2023, **13**, 2302429.

49. J. Zhou, B. Zhang, W. Zou, A. Tang, Y. Geng, Q. Zeng, Q. Guo and E. Zhou, *Sustain. Energ. Fuels.*, 2020, **4**, 5665-5673.

50. P. Guo, W. Miao, G. Liu, J. Tong, Q. Liang, Y. Zhang, C. Wang, E. Wang, H. Wu and Y. Xia, *Macromol. Chem. Phys.*, 2021, **222**, 2100030.